

LncRNA XIST Relieves Hypoxia-Induced Damage in H9C2 Cells by Downregulating miR-429

Na Yu
Xue Han
Xueqin Wang
Wanling Yu

Liqiu Yan

Na Yu¹Department one of cardiovascular medicine, Cangzhou Central Hospital, Cangzhou 061001, P.R.China, Xue Han²Department one of cardiovascular medicine, Cangzhou Central Hospital, Cangzhou 061001, P.R.China, Xueqin Wang³Department one of cardiovascular medicine, Cangzhou Central Hospital, Cangzhou 061001, P.R.China, Wanling Yu⁴Department one of cardiovascular medicine, Cangzhou Central Hospital, Cangzhou 061001, P.R.China, **Liqiu Yan**⁵Department one of cardiovascular medicine, Cangzhou Central Hospital, Cangzhou 061001, P.R.China, *Corresponding author: Department one of cardiovascular medicine, Cangzhou Central Hospital, No.16 Xinhua West Road, Cangzhou 061001, P.R.China (E-mail: 375011349@qq.com)

This paper aimed to investigate LncRNA XIST relieving hypoxia-induced damage in H9C2 cells by downregulating miR-429. Rat H9C2 cell lines were selected and divided into a normal control group, a hypoxia group, a XIST expression group, a XIST blank expression group, a miR-429 interference group and a blank interference group. qPCR was adopted for detecting LncRNA XIST and miR-429 expression. Western blot (WB) was adopted for detecting the expression of AMPK, PDH, FAT, MCPT-1, Caspase-3, Bax and Bcl-2, ATP content, and levels of SOD, MDA and LDH. Dual luciferase reporter gene assay (DLRGA) and RNA pull-down were adopted for verifying the correlation of LncRNA XIST with miR-429. Hypoxia-induced H9C2 cells had low LncRNA XIST expression and high miR-429 expression. LncRNA XIST upregulation or miR-429 downregulation could inhibit AMPK, PDH, Caspase-3 and Bax, upregulate FAT, MCPT-1 and Bcl-2, and increase ATP content and SOD activity, as well as reduce MDA content and LDH activity. miR-429 was the target gene of LncRNA XIST. LncRNA XIST can relieve hypoxia-induced damage in H9C2 cells via binding to and downregulating miR-429.

Keywords: LncRNA XIST; miR-429; hypoxia induction; myocardial cells; protective effect

Tob Regul Sci.™ 2021;7(5):1245-1253

DOI: doi.org/10.18001/TRS.7.5.41

INTRODUCTION

Myocardial ischemia (MI) is a cardiovascular disease (CVD) with the highest incidence and mortality rate across the world. According to statistics, the death toll from CVDs, among which ischemic cardiovascular disease is the most common type, accounts for approximately 1/3 of the world's deaths, and the data show a continuous growth trend (1). MI leads to deficiencies of myocardial oxygen supply and nutrients, thereby causing cardiac dysfunction and failure (2). As for the current treatment of ischemic cardiovascular disease, blood flow is mainly restored to reduce the ischemia-induced damage to the cardiovascular system, but the restoration also results in

ischemia-reperfusion injury and further aggravates myocardial damage (3). Decreased blood supply leads to cell apoptosis and necrosis. Apoptosis is a process jointly regulated by many factors, among which hypoxia is the most important cause of cell damage (4-6).

In human genomes, only 2% of nucleotide sequences are used for protein expression, and the vast majority of transcripts are non-coding RNAs (ncRNAs), a group of RNAs with a length of >200 nucleotides, no specific and complete open reading frame, and no protein-coding function. Although LncRNAs cannot encode proteins, they are important participants in gene regulation (7-8). ncRNAs are regulatory factors involved in many

LncRNA XIST Relieves Hypoxia-Induced Damage in H9C2 Cells by Downregulating miR-429

biological processes in CVDs, such as ischemic/hypoxic myocardial injury (9). Located in the inactivation center of X chromosome, XIST is encoded by the XIST gene of human Xq13.2, approximately 19 kb long in total. As a major regulator of mammalian X chromosome inactivation, it exerts a great function in the differentiation, proliferation and genome repair of human cells (10-11). According to recent studies, XIST is associated with ischemic myocardial injury and remarkably reduces in myocardial hypertrophy, which indicates that it has a therapeutic effect on myocardial cell dysfunction (12).

microRNAs, highly conserved ncRNAs approximately 18-24 nucleotides long, regulate translation mainly through binding to mRNAs' 3'-untranslated region (UTR), and readjust cell signal transduction pathways and proteins during cell development (13). Studies have shown that a series of intracellular and extracellular miRNAs changes are correlated with CVDs including myocardial infarction (14), myocardial hypertrophy (15) and arrhythmia (16). miR-429 belongs to miR-200 family, imbalanced in different types of cancers (17).

For exploring protective mechanisms of LncRNA XIST and miR-429 in hypoxic myocardial injury, H9C2 cells were treated with hypoxia in this study, and the two indicators' protective effects were observed, so as to provide support for the clinical application of LncRNAs or strategies for myocardial treatment based on miRNAs.

MATERIALS AND METHODS

Cell Culture

Purchased from ATCC, rat myocardial cells (H9C2) were placed in a complete DMEM, which contained 10% fetal bovine serum (FBS), penicillin (100 U/mL) and streptomycin (100 µg/mL), for culture in a cell incubator (37°C, 5% CO₂). They were digested and passaged at 1: 2 when fusing to 80%-90%, and the medium was changed at 24 hours after adherence.

qPCR

Trizol extraction kits (Invitrogen, USA) were adopted for drawing total RNA, whose optical density (OD) values were obtained at 260-280 nm using an ultraviolet spectrophotometer. The RNA was used for subsequent qPCR quantification if its OD₂₆₀/OD₂₈₀ was >1.8. XIST and miR-429 primers were designed and synthesized by Sangon Biotech (Shanghai) Co., Ltd. Forward and reverse sequences of the former were 5'-CCATTGAAGATACCACGCTGC-3' and 5'-GGTTGTTGCCAGGGTAGTG-3'. Those of the latter were

5'-CGGTAATACTGTCTGGTAA-3' and 5'-GTGCAGGGTCCGAGGT-3'. Next, the reverse transcription of RNA into cDNA was performed using PrimeScript RT kits, with a system of 10 µL, based on the kit instruction. The reaction conditions were 25°C for 30 min, 45°C for 30 min and 85°C for 5 min. Using cDNA as a template, fluorescence quantitative PCR was carried out with 2×TaqMan universal PCR Master Mix under the reaction conditions of 95°C for 3 min, cycling 5 times (94°C for 20 s, 63°C for 30 s, 72°C for 30 s) and cycling 40 times (95°C for 15 s, 60°C for 30 s), with U6 and β-actin being internal references of miR-429 and LncRNA XIST, respectively. Three same wells and negative controls without a template were set up for all reactions. Quantitative analysis was carried out by 2^{-ΔΔC_t} (12 additional same wells were set up for the correlation of LncRNA XIST with miR-429).

Cell Treatment and Transfection

H9C2 cells were inoculated into a 6-well plate and divided into the normal control group, the hypoxia group, the XIST expression group, the XIST blank expression group, the miR-429 interference group and the blank interference group. Cells in the four latter groups were respectively transfected with XIST overexpression plasmids, XIST overexpression plasmid blank controls, miR-429 inhibitor and miR-42 inhibitor blank controls. In the normal control group, the cells were cultured in normal oxygen (21% O₂, 5% CO₂, 74% N₂), while in the five latter groups, those were cultured in incubators (94% N₂, 5% CO₂, 1% O₂) for stimulating hypoxia injury. After 24-hour culture, follow-up related experiments were carried out.

Determination of Cell Viability

After transfection, the cells in each group were digested with trypsin and then inoculated into a 96-well plate, with the density adjusted to 4×10⁴ cells/well. Each group was provided with 6 same wells. The culture solution was discarded at 12, 24, 48 and 72 hours after culture (in the normal control group, those were cultured under normal oxygen, but in the five latter groups, those were cultured under hypoxia). A 0.5 g/L MTT solution (500 µL) was added to each well, for 4-hour incubation at 37°C in dark. After the supernatant was carefully absorbed, the mixture was added with DMSO solution (200 µL), shaken gently for 1 min in dark, and finally incubated for 10 min. OD values of each well at 490 nm were determined using a microplate reader.

Western Blot (WB)

RIPA lysis buffer (Solarbio) was used for

drawing total protein from the cells, and BCA protein assay was adopted for measuring the protein concentration and level it. After SDS gel electrophoresis, the PVDF membrane was cleaned with TBST solution, added with 5% milk blocking reagent, placed on a flat shaking table for slowly shaking, and finally sealed for 2 hours. After the membrane was removed and cleaned with TBST solution, the antibodies were incubated. The membrane was put into a hybridization bag and added with the diluted primary antibody. After air bubbles were carefully removed, the bag was sealed and shaken on the shaking table in a refrigerator (4°C), for incubation all night. The next day, the membrane was taken out and equilibrated at room temperature for 2 hours. After washed with TBST solution, it was put into a new hybridization bag and added with diluted secondary antibody. After sealing, the bag was placed on the table and gently shaken over 2 hours for incubation. After the membrane was cleaned with TBST solution, the gel imaging system was started to pre-cool to -20°C, with a preservative film spread and the film faced up. The equal volume of ECL luminescence reagent kits (substrates A and B) was taken out, and evenly dripped on the film after preparation, with the door closed for exposure. After that, the gel scanning imaging system was used for scanning and ChemiScope Analysis was used for analysis. The relative expression of the protein to be detected = the gray value of the band to be detected/the gray value of the β actin band, with β actin used as the internal reference protein. AMPK (adenosine monophosphate-activated protein kinase), PDH (pyruvate dehydrogenase), FAT (fatty acid), MCPT-1 (carnitine acyltransferase 1), Caspase-3, Bax, Bcl-2, β actin primary antibody and secondary antibody goat anti-rabbit (HRP cross-linked) were purchased from Cell Signaling Technology.

Detection of ATP Content and Oxidative Stress Factors

Supernatants of cell culture solution in each group were collected and centrifuged at 1000 r/min for 4 min, to obtain the upper layer culture solution. SOD, MDA and LDH activities in the supernatants were detected according to the instructions of SOD, MDA and LDH kits (purchased from MSK Biotechnology Co., Ltd., Wuhan). ATP content in the supernatants was detected according to ATP detection kits (purchased from Beyotime Biotechnology).

Flow Cytometry for Apoptosis Detection

Cells in each group were collected with the density adjusted to 2×10^6 cells/mL. The apoptosis was detected according to the instruction of FITC-Annexin V kits (Beyotime Biotechnology).

Dual Luciferase Reporter Gene Assay (DLRGA) and RNA Pull-down

LncRNA XIST and miR-429 were predicted for their binding sites. After digestion, H9C2 cells normally cultured in the logarithmic growth phase were inoculated into a 24-well culture plate (1×10^5 cells/well), for culture in an incubator (37°C, 5% CO₂), until the cell fusion was approximately 60% for transfection. XIST-WT 3'-UTR and XIST-MUT 3'-UTR vectors were constructed, and then respectively co-transfected with miR-429 mimic and NC mimic into the cells, based on the instruction of X-treme gene HP transfection reagents (purchased from Roche). Luciferase intensities were detected using the DLRGA system (Promega).

Biotin-labeled miR-429 WT and miR-429 MUT plasmids (50 nM each) were respectively transfected into the H9C2 cells. After 48 hours, the cells were collected, washed with PBS, and then incubated with specific cell lysis buffer (Ambion, Austin, Texas, USA) for 10 min. Subsequently, sample cell lysis buffer (50 mL) was subpackaged. The residual lysates were incubated with M-280 streptavidin magnetic beads (purchased from Sigma, St. Louis, MO, USA) that were precoated with RNase-free and yeast tRNA (purchased from Sigma, St. Louis, MO, USA). After 3-hour incubation at 4°C, the mixture was cleaned twice with cold lysates, three times with low-salt buffer and once with high-salt buffer. An antagonistic miR-429 probe was set up as a negative control. Total RNA was extracted with Trizol, and then LncRNA XIST expression was measured with qRT-PCR.

Statistics and Analysis

SPSS20.0 was used to statistically analyze the data. Measurement data were expressed by mean \pm SD, and independent samples t test was used for their comparison within groups, and ANOVA was used for the comparison between multiple groups. Count data were expressed by n(%), and chi-square test was used. GraphPad Prism8.0 was used to process the data.

RESULTS

Comparison of LncRNA XIST and miR-429 Expression and Activities

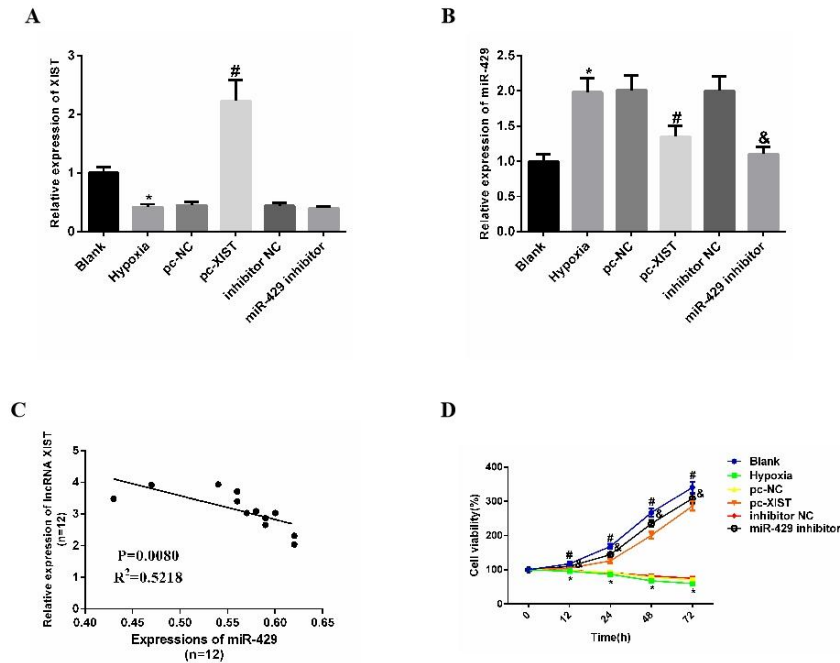
Compared with those cultured under normal oxygen, hypoxia-induced H9C2 cells had low LncRNA XIST expression and high miR-429 expression. LncRNA XIST rose but miR-429 reduced in H9C2 cells transfected with XIST overexpression plasmids and cultured under hypoxia ($P < 0.001$). LncRNA XIST was not significantly different but miR-429 remarkably

LncRNA XIST Relieves Hypoxia-Induced Damage in H9C2 Cells by Downregulating miR-429

reduced in H9C2 cells transfected with miR-429 interferents and cultured under hypoxia. The expression of the two indicators in H9C2 cells was significantly negatively correlated. The

determination was performed on cell viability, which remarkably reduced under the hypoxic environment but could be promoted after LncRNA XIST overexpression or miR-429 low-expression.

Figure 1
Comparison of LncRNA XIST and miR-429 expression and activities

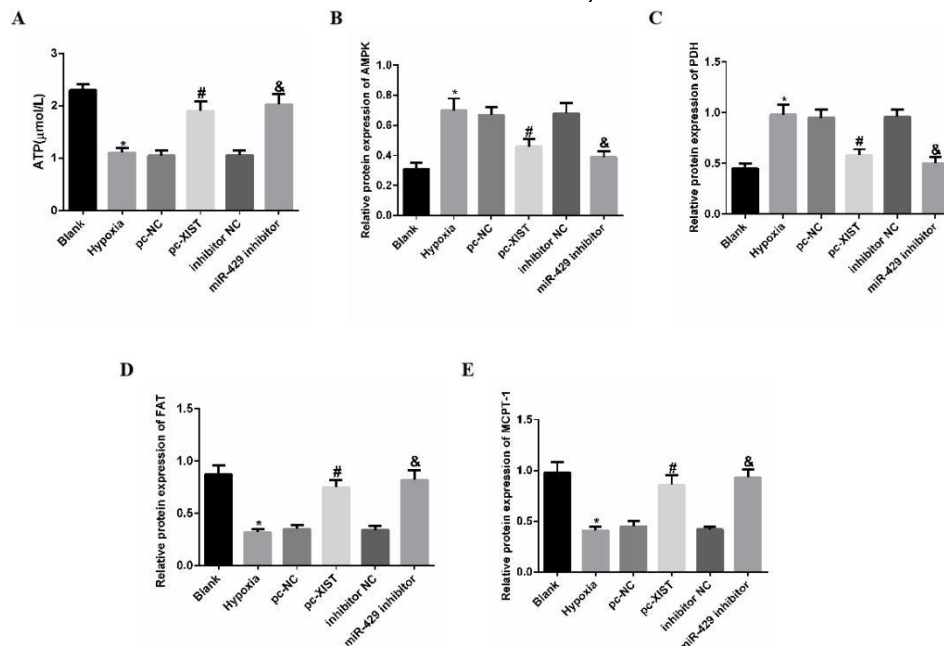


(A: LncRNA XIST expression in each group of cells. B: miR-429 expression in each group of cells. C: The correlation of LncRNA XIST with miR-429 expression in H9C2 cells. D: The comparison of cell viability between each group. * indicates $P < 0.001$ compared with the Blank group. # indicates $P < 0.001$ compared with the pc-NC group. & indicates $P < 0.001$ compared with the inhibitor NC group.)

Protein Contents Related to Myocardial Cells

ATP content and protein contents of FAT, MCPT-1, AMPK and PDH in myocardial cells remarkably reduced in the hypoxia group compared with the normal control group ($P < 0.001$). All of the indicators were remarkably improved in the pc-XIST and miR-429 inhibitor groups compared with the groups transfected with blank plasmids.

Figure 2
Protein contents related to myocardial cells



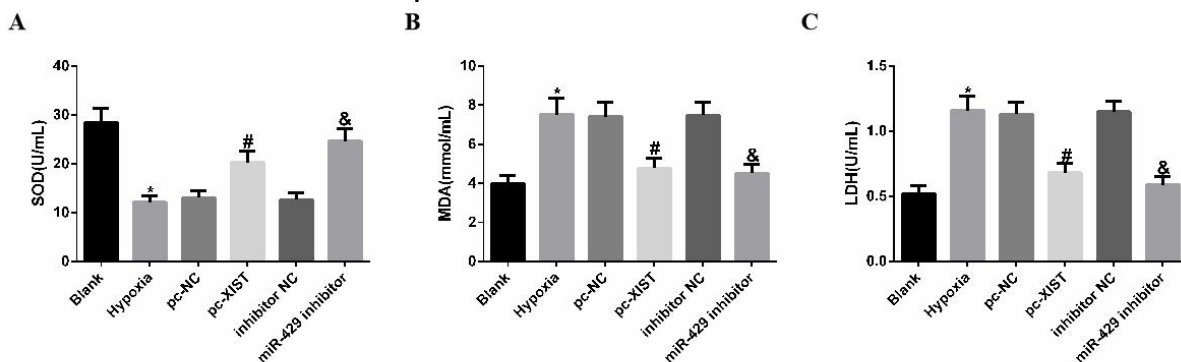
(A: The comparison of ATP content between each group. B: The comparison of AMPK protein content between each group. C: The comparison of PDH protein content between each group. D: The comparison of FAT protein content between each group. E: The comparison of MCPT-1 protein content between each group. * indicates $P < 0.001$ compared with the Blank group. # indicates $P < 0.001$ compared with the pc-NC group. & indicates $P < 0.001$ compared with the inhibitor NC group.)

Comparison of Oxidative Stress Indices

SOD activity reduced, but MDA level and LDH activity rose in the hypoxia group compared with the normal control group ($P < 0.001$). All of

the indicators were remarkably improved in the pc-XIST and miR-429 inhibitor groups compared with the hypoxia and blank transfection groups ($P < 0.001$).

Figure 3
Comparison of oxidative stress indices



(A: The comparison of SOD activity between each group. B: The comparison of MDA level between each group. C: The comparison of LDH activity between each group. * indicates $P < 0.001$ compared with the Blank group. # indicates $P < 0.001$ compared with the pc-NC group. & indicates $P < 0.001$ compared with the inhibitor NC group.)

Comparison of Cell Apoptosis

According to the flow cytometry, the apoptotic rate in the hypoxia group was remarkably

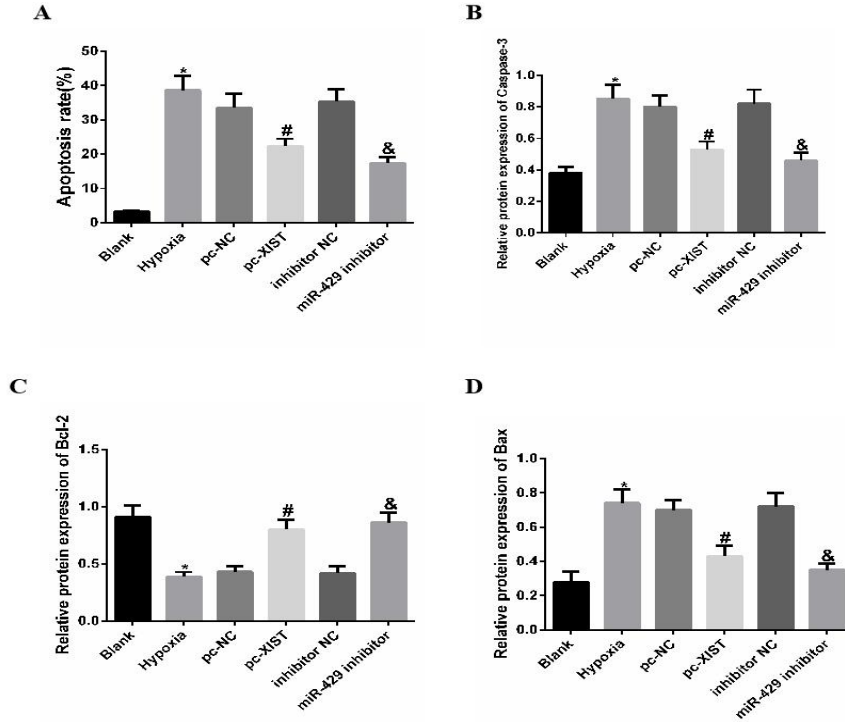
higher than that in the normal control group, and the rates in the pc-XIST and miR-429 inhibitor groups were remarkably lower than those in the

LncRNA XIST Relieves Hypoxia-Induced Damage in H9C2 Cells by Downregulating miR-429

hypoxia and blank transfection groups ($P < 0.001$). Bcl-2 protein expression remarkably reduced, but Bax and Caspase-3 protein expression remarkably rose in the hypoxia group compared with the

normal control group ($P < 0.001$). All of the indicators were remarkably improved in the pc-XIST and miR-429 inhibitor groups.

Figure 4
Comparison of cell apoptosis

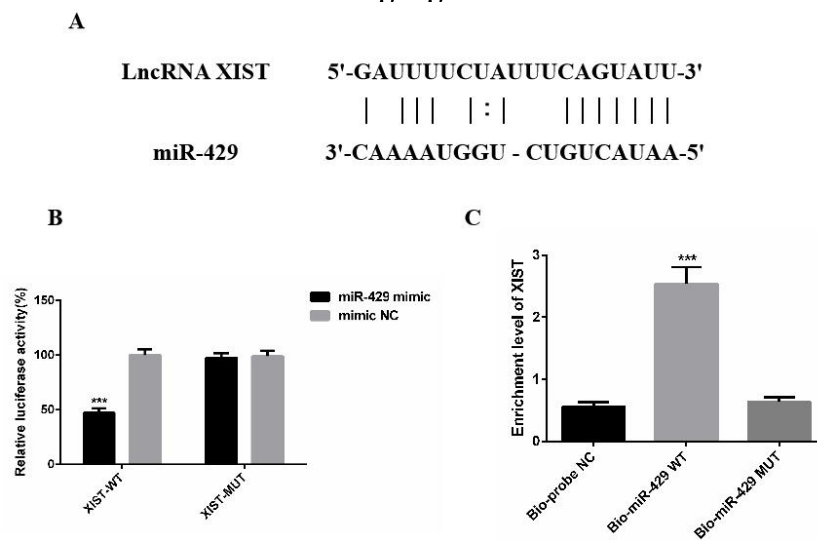


(A: The comparison of the apoptotic rate between each group. B: The comparison of Caspase-3 protein expression between each group. C: The comparison of Bcl-2 protein expression between each group. D: The comparison of Bax protein expression between each group. * indicates $P < 0.001$ compared with the Blank group. # indicates $P < 0.001$ compared with the pc-NC group. & indicates $P < 0.001$ compared with the inhibitor NC group.)

miR-429 Was the Target Gene of LncRNA XIST

According to the prediction by Starbase2.0, LncRNA XIST could be paired with and bind to miR-429 (Figure 5A). According to the DLRGA, luciferin activities reduced after XIST-WT and miR-429 mimic co-transfection, with no obvious changes after other co-transfection combinations (Figure 5B). According to the RNA pull-down, miR-429 could specifically bind to LncRNA XIST (Figure 5B). The above results reveal that LncRNA XIST can downregulate miR-429 by binding to this miR.

Figure 5
miR-429 was the target gene of LncRNA XIST



(A: LncRNA XIST could be paired with and bind to miR-429. B: DLRGA. C: RNA pull-down. *** indicates $P < 0.001$ compared with the NC group.)

DISCUSSION

Every year, approximately millions of people die from ischemic heart injury caused by hypoxia, which aggravates myocardial damage and apoptosis (2), so understanding the precise molecular mechanism of hypoxia-induced myocardial cell injury in clinical cardiovascular therapy is essential. In this paper, the protective effect of LncRNA XIST on hypoxic myocardial cells by downregulating miR-429 was studied, showing potential molecular targets for treating hypoxia-induced myocardial damage.

H9C2 cells were selected and induced for hypoxia, which showed that LncRNA XIST was lowly and miR-429 was highly expressed in the hypoxia-induced H9C2 cells. According to recent reports, LncRNA XIST rises in colon cancer (18) and gastric cancer (19), but reduces in breast cancer (20) and remarkably reduces in MI (12). miR-429 is abnormally expressed in colon cancer (21) and breast cancer (22). Subsequently, LncRNA XIST upregulation or miR-429 downregulation in myocardium was found to inhibit AMPK and PDH, upregulate FAT and MCPT-1, and increase ATP content. Under the hypoxic environment, ATP content reduces in myocardial cells, and energy required for myocardial cell metabolism mainly comes from mitochondria. The cells that fail under long-term ischemia and hypoxia are attacked by a large number of harmful substances, resulting in mitochondrial damage and accelerating heart failure (23). Mitochondria synthesize ATP through oxidative phosphorylation to supply energy

to various chemical reactions and functions in cells (24). LncRNA XIST upregulation or miR-429 downregulation can increase ATP content in hypoxia-induced myocardial cells, thus enhancing myocardial contractility and improving cardiac function. When heart failure occurs, substrates of myocardial energy metabolism change from the preferential use of FAT to glucose. During ischemia and hypoxia, pyruvate dehydrogenase (PDH) activation accelerates, leading to increased myocardial lactic acid, glucose oxidation and AMPK activity. MCPT-1 protein expression reduced in the hypoxia group, indicating that myocardial cells reduced the energy supply by FAT oxidation and decreased FAT transport under the hypoxic environment. LncRNA XIST upregulation or miR-429 downregulation can increase FAT and MCPT-1 expression in hypoxia-induced myocardial cells, thereby increasing FAT metabolism. It also increases SOD activity and reduces MDA content and LDH activity. Oxidative stress is another important mechanism of hypoxia-induced myocardial cell injury, also one of the earliest injury mechanisms of ischemic cardiovascular disease (25). SOD is the body's first line of defense against oxidative stress, whose occurrence is inhibited by SOD upregulation (26). LncRNA XIST upregulation or miR-429 downregulation can increase cell activity, inhibit Caspase-3 and Bax, upregulate Bcl-2, and reduce the apoptotic rate of myocardial cells. Studies have shown that the hypoxic environment induces endoplasmic reticulum stress (ERS), whose inhibition promotes myocardial cells' survival and inhibits their

LncRNA XIST Relieves Hypoxia-Induced Damage in H9C2 Cells by Downregulating miR-429

apoptosis (27). Three main pathways, including exogenous pathways involving death protein receptors and endogenous pathways of mitochondria and endoplasmic reticulum, regulate apoptosis or programmed cell deaths (28). Mitochondrial pathways are mainly mediated by members of the Bcl-2 family and cause cell damage (such as DNA damage and cell distress), thus damaging mitochondria to release mediators (such as apoptosis-inducing factors and cytochrome C) into cytoplasm and eventually inducing caspase cascade activation (29). Finally, miR-429 was confirmed as the target gene of LncRNA XIST.

In summary, hypoxia-induced H9C2 cells have low LncRNA XIST expression and high miR-429 expression. LncRNA XIST upregulation and miR-429 downregulation can protect hypoxic myocardial cells, enhance cell activity, and inhibit cell apoptosis, so as to provide support for the clinical application of LncRNAs.

REFERENCES

1. Tibaut Miha, Mekis Dusan, Petrovic Daniel, Pathophysiology of Myocardial Infarction and Acute Management Strategies.[J]. *Cardiovasc Hematol Agents Med Chem*, 2017, 14: 150-159.
2. Schreiber Timm, Salhofer Luca, Quinting Theresa. Things get broken: the hypoxia-inducible factor prolyl hydroxylases in ischemic heart disease.[J]. *Basic Res. Cardiol.*, 2019, 114: 16.
3. Hortmann Marcus, Robinson Samuel, Mohr Moritz. The mitochondria-targeting peptide elamipretide diminishes circulating HtrA2 in ST-segment elevation myocardial infarction.[J]. *Eur Heart J Acute Cardiovasc Care*, 2019, 8: 695-702.
4. Simmen Simona, Cosin-Roger Jesus, Melhem Hassan. Iron Prevents Hypoxia-Associated Inflammation Through the Regulation of Nuclear Factor- κ B in the Intestinal Epithelium.[J]. *Cell Mol Gastroenterol Hepatol*, 2019, 7: 339-355.
5. Arngrim Nanna, Hougaard Anders, Schytz Henrik W. Effect of hypoxia on BOLD fMRI response and total cerebral blood flow in migraine with aura patients.[J]. *J. Cereb. Blood Flow Metab.*, 2019, 39: 680-689.
6. Prabhakar N R , Semenza G L . Adaptive and Maladaptive Cardiorespiratory Responses to Continuous and Intermittent Hypoxia Mediated by Hypoxia-Inducible Factors 1 and 2[J]. *Physiological Reviews*, 2012, 92(3):967-1003.
7. Uchida S , Dimmeler S . Long Noncoding RNAs in Cardiovascular Diseases[J]. *Circulation Research*, 2015, 116(4):737-750.
8. Sun Ningning, Zhang Guozun, Liu Yingying, Long non-coding RNA XIST sponges miR-34a to promotes colon cancer progression via Wnt/ β catenin signaling pathway.[J]. *Gene*, 2018, 665: 141-148.
9. Ying H . The novel regulatory role of lncRNA-miRNA-mRNA axis in cardiovascular diseases[J]. *Journal of Cellular & Molecular Medicine*, 2018.
10. Sahakyan Anna, Yang Yihao, Plath Kathrin, The Role of Xist in X-Chromosome Dosage Compensation.[J]. *Trends Cell Biol.*, 2018, 28: 999-1013.
11. Loda Agnese, Heard Edith, Xist RNA in action: Past, present, and future.[J]. *PLoS Genet.*, 2019, 15: e1008333.
12. Peng Hui, Luo Yuxuan, Ying Yongjun, lncRNA XIST attenuates hypoxia-induced H9c2 cardiomyocyte injury by targeting the miR-122-5p/FOXP2 axis.[J]. *Mol. Cell. Probes*, 2020, 50: 101500.
13. Lu Thomas X, Rothenberg Marc E, MicroRNA.[J]. *J. Allergy Clin. Immunol.*, 2018, 141: 1202-1207.
14. Gabisonia Khatia, Prosdocimo Giulia, Aquaro Giovanni Donato. MicroRNA therapy stimulates uncontrolled cardiac repair after myocardial infarction in pigs.[J]. *Nature*, 2019, 569: 418-422.
15. Wehbe N , Nasser S A , Pintus G ., MicroRNAs in Cardiac Hypertrophy[J]. *International Journal of Molecular Sciences*, 2019, 20(19):4714.
16. Cheng Wan-Li, Kao Yu-Hsun, Chao Tze-Fan. MicroRNA-133 suppresses ZFX3-dependent atrial remodelling and arrhythmia.[J]. *Acta Physiol (Oxf)*, 2019, 227: e13322.
17. Huang Guo-Liang, Sun Jiancong, Lu Yan. MiR-200 family and cancer: From a meta-analysis view.[J]. *Mol. Aspects Med.*, 2019, 70: 57-71.
18. Sun Ningning, Zhang Guozun, Liu Yingying, Long non-coding RNA XIST sponges miR-34a to promotes colon cancer progression via Wnt/ β catenin signaling pathway.[J]. *Gene*, 2018, 665: 141-148.
19. Zhang Quan, Chen Baiyu, Liu Ping. XIST promotes gastric cancer (GC) progression through TGF- β via targeting miR-185.[J]. *J. Cell. Biochem.*, 2018, 119: 2787-2796.
20. Xing Fei, Liu Yin, Wu Shih-Ying. Loss of XIST in Breast Cancer Activates MSN-c-Met and Reprograms Microglia via Exosomal miRNA to Promote Brain Metastasis.[J]. *Cancer Res.*, 2018, 78: 4316-4330.
21. Santasusagna Sandra, Moreno Isabel, Navarro Alfons. Prognostic Impact of miR-200 Family Members in Plasma and Exosomes from Tumor-Draining versus Peripheral Veins of Colon Cancer Patients.[J]. *Oncology*, 2018, 95: 309-318.
22. Dai Wenzhu, He Jixiang, Zheng Ling. miR-148b-3p, miR-190b, and miR-429 Regulate Cell Progression and Act as Potential Biomarkers for Breast Cancer.[J]. *J Breast Cancer*, 2019, 22: 219-236.
23. Facundo Hebert di Tarso Fernandes, Brainard Robert Eli, Caldas Francisco Rodrigo de Lemos. Mitochondria and Cardiac Hypertrophy.[J]. *Adv. Exp. Med. Biol.*, 2017, 982: 203-226.
24. Lopaschuk G D , Ussher J R . Evolving Concepts of Myocardial Energy Metabolism: More Than Just Fats and Carbohydrates[J]. *Circulation Research*, 2016, 119(11):1173-1176.
25. Wei Wenjuan, Peng Jun, Li Jian, Curcumin attenuates hypoxia/reoxygenation-induced myocardial

Na Yu et al.

LncRNA XIST Relieves Hypoxia-Induced Damage in H9C2 Cells by Downregulating miR-429

injury.[J] .Mol Med Rep, 2019, 20: 4821-4830.

26. Sun Lei,Zang Wei-Jin,Wang Hao. Acetylcholine promotes ROS detoxification against hypoxia/reoxygenation-induced oxidative stress through FoxO3a/PGC-1 α dependent superoxide dismutase.[J] .Cell. Physiol. Biochem., 2014, 34: 1614-25.
27. Li Wenyuan,Li Wei,Leng Yan. Ferroptosis Is Involved in Diabetes Myocardial Ischemia/Reperfusion Injury Through Endoplasmic Reticulum Stress.[J] .DNA Cell Biol., 2020, 39: 210-225.
28. D'Arcy Mark S,Cell death: a review of the major forms of apoptosis, necrosis and autophagy.[J] .Cell Biol. Int., 2019, 43: 582-592.
29. Chen Xin,Chen Long,Jiang Shanxiang. Maduramicin induces apoptosis and necrosis, and blocks autophagic flux in myocardial H9c2 cells.[J] .J Appl Toxicol, 2018, 38: 366-375.